

Overmerging and M/L ratios in phenomenological galaxy formation models

Eelco van Kampen^{1,2}, Raul Jimenez¹ and John A. Peacock¹

¹ *Institute for Astronomy, University of Edinburgh, Royal Observatory, Blackford Hill, Edinburgh EH9 3HJ*

² *Theoretical Astrophysics Center, Juliane Maries Vej 30, DK-2100 Copenhagen Ø, Denmark*

Accepted ... Received ...; in original form ...

ABSTRACT

We show that the discrepancy between the Tully-Fisher relation and the luminosity function predicted by most phenomenological galaxy formation models is mainly due to overmerging of galaxy haloes. We have circumvented this overmerging problem, which is inherent in both the Press-Schechter formalism and dissipationless N-body simulations, by including a specific galaxy halo formation recipe into an otherwise standard N-body code. This numerical technique provides the merger trees which, together with simplified gas dynamics and star formation physics, constitute our implementation of a phenomenological galaxy formation model. Resolving the overmerging problem provides us with the means to match both the I-band Tully-Fisher relation and the B and K band luminosity functions within an $\Omega = 1$ Λ CDM structure formation scenario. It also allows us to include models for chemical evolution and starbursts, which improves the match to observational data *and* renders the modelling more realistic. We show that the inclusion of chemical evolution into the modelling requires a significant fraction of stars to be formed in short bursts triggered by merging events.

Key words: cosmology: theory - dark matter - large-scale structure of Universe - galaxy formation

1 INTRODUCTION

There has been significant recent progress in the study of galaxy formation within a cosmological context, mainly due to a phenomenological or ‘semi-analytical’ approach to this problem. The idea is to start with a structure formation model that describes where and when galactic dark haloes form. A simple description of gas dynamics and star formation provides a means to calculate the amount of stars forming in these haloes. Stellar population synthesis models then provide the spectral evolution, i.e. luminosities and colours, of these galaxies.

Many physical processes are modelled as simple functions of the circular velocity of the galaxy halo. Therefore, the Tully-Fisher relation is the most obvious observational relation to try and predict, as it relates the total luminosity of a galaxy to its halo circular velocity. However, most phenomenological galaxy formation models do not simultaneously fit the I-band Tully-Fisher relation and the B or K band luminosity function. When one sets the model parameters such that the Tully-Fisher relation has the right normalization, the luminosity functions generally overshoot (e.g. Kauffman, White & Guiderdoni 1993; Kaufmann, Colberg, Diaferio & White 1998), certainly for the $\Omega = 1$, $H_0 = 50$ $\text{km s}^{-1} \text{Mpc}^{-1}$ standard CDM cosmology (in the form given

by Davis et al. 1985) that we consider in this paper. Alternatively, when making sure that the luminosity functions matches by changing some of the model parameters, the Tully-Fisher relation ends up significantly shifted with respect to the observed relation (e.g. Cole et al. 1994; Heyl et al. 1995).

In order to keep the modelling as analytical as possible, an extension to the Press & Schechter (1974) prescription for the evolution of galaxy haloes (e.g. Bond et al. 1991; Bower 1991; Lacey & Cole 1993; Kauffman & White 1993) has been a popular ingredient for implementations of a phenomenological theory of galaxy formation. The extended Press-Schechter (EPS) formalism keeps the galaxy formation model as analytical as possible, and allows fast realizations of halo populations. However, this prescription has the disadvantage that the large-scale phase-space distribution of haloes is unknown, as is any information on their internal structure and kinematics. For many applications this information will be of great use. Furthermore, the properties and formation histories of *individual* haloes do not match the corresponding properties and histories as predicted by the EPS formalism (e.g. Lacey & Cole 1993; White 1996).

More importantly, the EPS formalism is designed to identify collapsed systems, irrespective of whether these contain surviving subsystems. This ‘overmerging’ of subhaloes

into larger embedding haloes produces a top-heavy galaxy halo mass function, and is therefore relevant to the problem of matching both the luminosity function and the Tully-Fisher relation. Traditional N-body simulations suffer from a similar overmerging problem (e.g. White 1976), which is of a purely numerical nature, caused by two-body heating in dense environments (Carlberg 1994; van Kampen 1995) when the mass resolution is too low. This is why the statistical properties of EPS haloes and haloes found in N-body simulations still agree quite well (e.g. Efstathiou et al. 1988; Somerville et al. 1998 and references therein), despite the overmerging.

In order to circumvent these problems, we use an N-body simulation technique that includes a built-in recipe for galaxy halo formation, designed to prevent overmerging (van Kampen 1995, 1997), to generate the halo population and its formation and merger history. We show that this alone significantly changes the predictions for the Tully-Fisher relation and the luminosity function. In fact, it resolves most of the discrepancy sketched above, *and* allows us to make the modelling more realistic by adding chemical evolution and a merger-driven bursting mode of star formation to the modelling.

Star formation and its feedback to the interstellar medium are the least understood ingredients of theories of galaxy formation. Usually one considers a single mode of star formation, being either a continuous but decaying rate of star formation from gas that cools within dark haloes, or a discontinuous, bursting mode of star formation where stars are formed at a high rate in short periods. Here we will consider both, where the continuous mode of star formation encompasses the case of many short bursts of star formation. We reserve the term ‘starburst’ for single major starburst events, lasting on the order of 0.1 Gyr, as observed in luminous infrared galaxies, for example (Sanders & Mirabel 1996).

Once stars are formed, we apply the stellar population synthesis models of Jimenez et al. (1998) to follow their evolution. We have enhanced these models with a model for the evolution of the average metallicity of the population, which depends on the starting metallicity. Feedback to the surrounding material means that cooling properties of that material will change with time, affecting the star formation rate, and thus various other properties of the parent galaxy.

Several of our ingredients are thus different from earlier work: we use numerical simulations for the formation and evolution of the galaxy haloes, and we use newer population synthesis models, which include chemical evolution. Nevertheless, it is still useful to start from a model that is as similar as possible to a published one. This allows us to assess the changes in the model results due to the differences in modelling. We chose use the model of Cole et al. (1994) as a starting point.

The lay-out of this paper is as follows: we first discuss the main problems in Section 2, focusing on the overmerging of galaxy haloes, and ways of resolving the problems. In Section 3 we generate distributions of galaxies for which we calculate luminosity functions and the Tully-Fisher relation. We compare these to those found in previous work, and to observed ones. We discuss the interpretation of the results, pitfalls, and possible extensions, in the final section.

2 THE PHENOMENOLOGICAL MODEL FOR GALAXY FORMATION

In this section, we summarize how galaxy formation is modelled in this work. In many respects, we deliberately follow the approach of other groups, so as to aid comparison of results. Nevertheless, our methods differ in some important respects, as outlined below. A detailed discussion of the modelling is given in Appendix A; this section is intended as an overview for non-specialists.

2.1 Overview

The key ingredients of the model are:

- (1) *The merging history of dark-matter haloes.* This is often treated by Monte-Carlo realizations of the analytic ‘extended Press-Schechter’ formalism. That formalism is a successful description of collapsed systems with densities of order 200 times the mean, and of the history of merging that produced such systems. However, the theory ignores substructure: a cluster-scale halo is treated as a single system. The alternative is to measure halo substructure directly via N-body simulation. Special techniques are used in this paper to prevent galaxy-scale haloes undergoing ‘overmerging’ owing to inadequate numerical resolution. By allowing substructure to survive, the merger history is simplified and the number of halo mergers is reduced.
- (2) *The merging of galaxies within dark-matter haloes.* Each halo contains a single galaxy at formation. When haloes merge, a criterion based on dynamical friction is used to decide how many galaxies exist in the newly merged halo. The most massive of those galaxies becomes the single central galaxy to which gas can cool, while the others become its satellites. This approximate argument is one of the more uncertain parts of phenomenological galaxy formation schemes. We still use the dynamical friction method, but our treatment of halo overmerging means that part of the galaxy merging process is treated directly. This should make our results more robust.
- (3) *The history of gas within dark-matter haloes.* When a halo first forms, it is assumed to have an isothermal-sphere density profile. A fraction Ω_b/Ω of this is in the form of gas at the virial temperature, which can cool to form stars within a single galaxy at the centre of the halo. Application of the standard radiative cooling curve shows the rate at which this hot gas cools below 10^4 K, and is able to form stars. Energy output from supernovae reheats some of the cooled gas back to the hot phase. When haloes merge, all hot gas is stripped and ends up in the new halo. Thus, each halo maintains an internal account of the amounts of gas being transferred between the two phases, and consumed by the formation of stars.
- (4) *Quiescent star formation.* This is one of the more difficult areas to model. Most authors assume a star-formation timescale that is linearly proportional to the circular velocity of the dark-matter halo in which the galaxy sits. The star formation rate is equal the ratio of the amount of cold gas available and the star-formation

timescale. The amount of cold gas available depends on the merger history of the halo, the star formation history, and the how much cold gas has been reheated by feedback processes (discussed below).

- (5) *Starbursts.* We also introduce the idea that the star-formation rate may suffer a sharp spike following a major merger event. This is motivated empirically by the existence of ultra-luminous IRAS galaxies, and it allows hierarchical models to yield behaviour resembling traditional monolithic collapse. Our specific starburst model is described in Appendix B.
- (6) *Feedback from star-formation.* The energy released from young stars heats cold gas in proportion to the amount of star-formation, returning it to the reservoir of hot gas. This ingredient is essential to keep low-mass galaxies and proto-galaxies from using up all their gas at high redshift.
- (7) *Stellar evolution and populations.* Having formed stars, we wish to predict the appearance of the galaxy that results. For this, it is necessary to assume an IMF, and to have a spectral synthesis code. Our work assumes the spectral models of Jimenez et al. (1998); for solar metallicity, the results are not greatly different from those of other workers. The IMF is generally taken to be Salpeter, but any choice is possible. Unlike other workers, we take it as established that the population of brown dwarfs makes a negligible contribution to the total stellar mass density, and we do not allow an adjustable M/L ratio, Υ , for the stellar population.
- (8) *Chemical evolution.* It would of course be unrealistic to assume that the entire star-formation history of a galaxy can unfold at constant metallicity. The evolution of the metals must be followed, for two reasons: (i) the cooling of the hot gas depends on metal content; (ii) for a given age, a stellar population of high metallicity will be much redder. The models of Jimenez et al. (1998) allow synthetic stellar populations of any metallicity to be constructed. Appendix C discusses how the chemical evolution of the gas is followed.

2.2 Model parameters

This framework is rather general, and includes a number of parameters. Note that there are also parameters involved in the cosmological model. In this paper, we consider only a single variant of CDM ($\Omega = 1$, $h = 0.5$, $n = 1$, $\Omega_b = 0.06$, $\sigma_8 = 0.62$), in order to illustrate the effects of changes in the galaxy-formation model. This cosmological model is identical to the one used by Cole et al. (1994).

The equations containing the specific parameterizations of the above assumptions are given in Appedix A. The values assumed for these parameters in the models investigated in this paper are given in Table 1.

3 THE TULLY-FISHER / LUMINOSITY FUNCTION DISCREPANCY

Matching both the Tully-Fisher relation, which relates the infrared rest-frame magnitude to the circular velocity V_c of the halo, and the B-band luminosity function has been a

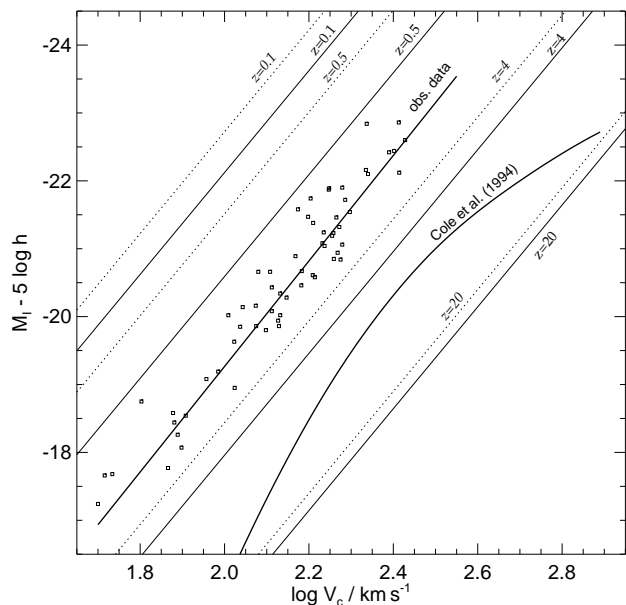


Figure 1. The Tully-Fisher relation: observational data and a simple model: single redshift collapse, with all available gas forming stars in an 0.1 Gyr burst (solid lines), or continuously with an exponential decay-time of 10 Gyr (dotted lines). The squares are individual galaxies as observed by Tully et al. (1998), whereas the thick straight line is an average over four fits to observational data by four different authors (see text for details). The thick curved line is a fit to the model of Cole et al. (1994, curve taken from Heyl et al. 1995). Note that the models of CAFNZ do have significant star formation up to the present epoch.

problem for most published phenomenological galaxy formation scenarios. In the following we use, as a starting point, the models of Cole et al. (1994, CAFNZ from here on), which show this discrepancy as well. When CAFNZ set their free parameters to match the B-band luminosity function, they did not find a good match to the I-band Tully-Fisher relation: it is either a factor of two too large in V_c , or 2-3 magnitudes too faint in I.

We believe that this is largely due to an excess of bright galaxies with rather large circular velocities, caused by overmerging within the (extended) Press-Schechter formalism used by CAFNZ. Because of the overabundance of massive galaxies, CAFNZ were forced to put in place several ‘brakes’ in order to prevent the luminosity evolution from overshooting. Firstly, they adopt a value for the star-formation timescale τ_*^0 which is half that of the value of 4 Gyr that is found in the numerical simulations of Navarro & White (1993), on which CAFNZ based their star formation models, and which was used to set many other parameters. Secondly, they adopted a very large mass-to-light ratio for the stellar population: they set $\Upsilon = 2.7$, where Υ is defined as the ratio of all stars to that of stars above $0.1 M_\odot$. Finally, they assume that all hot gas has primordial metallicity (even gas reheated by solar metallicity supernovae), which means it cools less rapidly than enriched gas and results in less stars being formed per unit mass. They also assumed instant enrichment to solar metallicity for their stellar populations, which helps keep the B-band magnitudes faint.

Table 1. Parameters for the phenomenological galaxy formation models discussed in Section 2, 3, and Appendix A.

Description	parameter	CAFNZ	m	n	c	s	a	b
Mass-to-light ratio:								
cosmological baryon fraction	Ω_b	0.06	0.06	0.06	0.06	0.06	0.06	0.06
$M(\text{all stars})/M(m > 0.1M_\odot)$	Υ	2.7	1.0	1.0	1.0	1.0	1.0	1.0
Continuous star formation:								
basic star formation time-scale	τ_*^0	2	2	2	2	10^6	2	2
power-law index	α^*	-1.5	-1.5	-1.5	-1.5	-1.5	-1.5	-0.5
Bursting star formation:								
basic star formation time-scale	τ_b^0	-	-	-	-	0.01	0.01	0.01
burst factor	f_b	-	-	-	-	10^6	100	100
Feedback (reheating of cooled gas by supernovae):								
feedback parameter	f_v	0.2	0.2	0.2	0.2	0.2	0.2	0.04
feedback normalization	V_{hot}	140	140	140	140	140	140	100
feedback power-law index	α_{hot}	5.5	5.5	5.5	5.5	5.5	5.5	4.0
Galaxy merging within haloes:								
dynamical friction time-scale	τ_{mrg}^0	$0.5\tau_{\text{dyn}}$	$0.5\tau_{\text{dyn}}$	$0.5\tau_{\text{dyn}}$	$0.5\tau_{\text{dyn}}$	$0.5\tau_{\text{dyn}}$	$0.5\tau_{\text{dyn}}$	$0.5\tau_{\text{dyn}}$
dynamical friction scaling law	α_{mrg}	0.25	0.25	0.25	0.25	0.25	0.25	0.25
Stellar populations:								
initial mass function	IMF	Scalo	Salpeter	Salpeter	Salpeter	Salpeter	Salpeter	Salpeter
metallicity	Z	solar	solar	solar	evolving	evolving	evolving	evolving

3.1 Building blocks for the Tully-Fisher relation

In order to provide a frame of reference for interpreting and understanding the Tully-Fisher relation produced by our models, we first greatly simplify the modelling by only incorporating some of the ingredients. The very simplest model is one in which a galaxy turns all its gas into stars at a single epoch of formation, either in a short burst of star formation, or as an exponentially decaying, but continuous star formation mode. We will refer to this type of model as a ‘single redshift star formation model’. The circular velocity is calculated using the spherical collapse model (e.g. Peebles 1980), where the density at first collapse is 178 times the background value, which gives $L \propto M_{\text{gas}} \propto V_c^3(1 + z_{\text{form}})^{3/2}$.

In Fig. 1 we plot the resulting Tully-Fisher relation for such a model, where the single formation redshift (for all galaxies) is annotated for each of the model relations. The straight thick solid line is an average of fits to four datasets (Pierce & Tully 1992; Mould et al. 1993 and references therein; Giovanelli et al. 1997; Mathewson, Ford & Buchhorn 1992), whereas the squares show the data of Young (1994), in order to give an indication of the typical spread around the observed relation. This average relation corresponds to $L \propto V_c^{3.1}$, so very close to that predicted by the spherical collapse model. The most obvious lesson to learn from this figure is that we can reproduce the Tully-Fisher relation simply by forming all galaxies between a redshift of 0.5 and 4, with a peak near $z = 1 - 2$, and turning all available gas into stars shortly after the formation event. Galaxies will move straight down in the diagram if only part of the gas is used up, so late star formation from a fraction of the gas produces the same relation as turning all gas into stars at early times.

3.2 Observed luminosity functions

In the models of CAFNZ the B and K-band luminosity function (LF for short) were used to set some of their free parameters, so that they matched well to the observed luminosity functions known at the time: the B-band LF of Loveday et al. (1992) and the K-band LF of Mobasher et al. (1986). Present day datasets show quite a change in the observed LF: Zucca et al. (1997) observe a much steeper faint end for the B-band LF, while Gardner et al. (1997) and Glazebrook et al. (1995) observe a K-band LF that is fainter at the bright end, although there is some disagreement at the faint end. It must be gratifying to CAFNZ that their models are closer to these new results than to the data of Loveday et al. (1992) and Mobasher et al. (1986). The significant discrepancy with the Tully-Fisher relation remains, however, and we attempt to resolve that in the remainder of this Section.

3.3 The galaxy halo population

3.3.1 Defining haloes

In most phenomenological galaxy formation recipes published so far the galaxy halo population and its formation and merger history are obtained from the extended Press-Schechter (EPS) formalism (see the introduction for references and discussion). It is essential to realize that the EPS formalism deals only with systems of density approximately 200 times the mean, which are *assumed* to be virialized. Such sets of particles are readily identified in N-body simulations e.g. by linking particles via the percolation (a.k.a. ‘friends-of-friends’) algorithm. Indeed, the term ‘halo’ is not infrequently taken implicitly to denote only systems of this sort. However, we feel this is an unfortunate useage, and we will use the term in this paper in a more general sense: as a virialized local density maximum. A rich cluster is an EPS halo, but the galaxies it contains are defined by dark-matter

haloes that constitute substructure in the cluster dark matter. These systems collapsed before the cluster, and so have present-day density contrasts well above 200. As the cluster forms, the outer parts of these galaxy-scale haloes merge and lose their identity; the high-density cores of the haloes will nevertheless survive and remain virialized, and mark the locations of galaxies within the cluster. The aim of a galaxy formation model is to predict the stellar content of these ‘embedded’ galaxy-scale haloes.

3.3.2 Overmerging

If one takes the galaxy haloes merger history from the EPS formalism, all embedding haloes are retained, but embedded haloes are lost; EPS records only when haloes are incorporated into a larger system, but subsequent evolution within the new system is not followed. We adopt the term ‘overmerging’ to describe this loss of information concerning the substructure in embedding haloes.

The use of the EPS formalism is usually motivated by the fact that the distribution of masses of the haloes and their formation histories are in good agreement with those found in N-body simulations (Efstathiou et al. 1988; Somerville et al. 1998 and references therein). However, this result depends on the choice of the group finder adopted to identify haloes in the simulations (Suginohara & Suto 1992). The usual choice is percolation with a fixed linking-length, which shares with the EPS formalism the property that embedded haloes are not identified. It also identifies *any* overdense group, not just virialized haloes.

Furthermore, overmerging also occurs in the N-body simulations to which the EPS formalism is compared. Small groups of particles that represent galaxy haloes get disrupted by numerical two-body heating, especially in large overdense systems (Carlberg 1994; van Kampen 1995). If the numerical resolution is good enough, this problem is resolved (Moore et al. 1998; Tormen, Diaferio & Syer 1998), but both the spatial and mass resolution need to be rather high: Klypin, Gottl ber & Kravtsov (1997) find that haloes survive for resolutions of a few kpc and 10^8 - $10^9 M_\odot$ respectively. Unfortunately, for N-body simulations on a cosmological scale, this requires the use of far too many particles (on the order of 10^9) to be practical, so a special N-body technique is needed instead.

3.3.3 Resolving the overmerging problem

In order to prevent overmerging, we adopt a simulation technique in which a galaxy halo formation recipe is added to an otherwise standard N-body technique (van Kampen 1995, 1997). The idea is that a group of particles that has collapsed into a virialised system with a mass appropriate of a galactic halo is replaced by a single ‘halo particle’. Local density percolation, also called adaptive friends-of-friends, is adopted for finding the groups (van Kampen 1997). This is designed to identify the embedded haloes that the traditional percolation group finder links up with their parent halo. A Gaussian filter, with a length equal to the average nearest neighbour distance for a Poisson particle distribution, is applied to calculate a local density n_G . This local density is then used to calculate a local linking length for the percolation algorithm, scaling as $n_G^{-1/3}$. The linking length

also scales with the particle mass m as $m^{1/2}$, in order to account for the larger gravitational pull of the more massive halo particles. The basic linking length (for mean density and non-halo particles) is half the Poissonian average nearest neighbour distance.

The virial equilibrium criterion is put into a simplified form using the half-mass radius R_h , motivated by Spitzer (1969) who found that for many equilibrium systems

$$\langle v^2 \rangle \approx 0.4 \frac{GM}{R_h}. \quad (1)$$

A group is considered to be virialized when this criterion is satisfied with a margin of 25 per cent. The new halo particle is softened according to the size of the group it replaces (thus conserving energy), and gets the position and momentum of the centre-of-mass of the original group. Because groups of particles can contain halo particles, merging is naturally included in this recipe as well. Note that we do *not* assume that each halo particle hosts a single galaxy. At formation, each halo particle may contain several pre-existing galaxies, and the dynamical friction argument (ingredient 2 of Section 2.1) has to be invoked to see whether they merge. However, our procedure clearly treats a good part of the general merging of galaxies directly, which increases the robustness of the results.

If groups are sufficiently massive compared to the numerical resolution of the code, they will avoid spurious numerical disruption in future evolution of the density field. There is therefore no need to replace these systems by a single particle. In fact, doing so would pose numerical problems as supermassive simulation particles will interact violently with ‘normal’ N-body particles. Therefore, an upper limit should be set to the mass of a halo particle.

However, the local density percolation group-finder we adopt here has been designed to identify haloes in the field as well as in overdense regions. This means that a smooth cluster containing no subhaloes will be identified as one massive halo, while a cluster many subhaloes will not be identified as a single halo. The centre of the cluster and the subhaloes will all be identified as separate entities. This implies that there will automatically be a maximum for the mass of the groups found, depending on the environment. This is discussed in more detail in van Kampen (1999, in preparation).

Preferably the upper limit to the halo particle-mass should equal this maximum group-mass, but as it depends on the group finder parameters, it is hard to predict its value. The results should be robust with respect to reasonable variations in this number, so the actual choice is not too important. We set the upper mass limit to be $7 \times 10^{13} h^{-1} M_\odot$, or about 1600 of the initial simulation particles.

3.3.4 Our halo population

We performed two high-resolution simulations, using the methods described above, with a (spherical) volume of $(23.2h^{-1}\text{Mpc})^3$, using around 8×10^5 particles. The first simulation started from initial conditions constrained to form a galaxy cluster in the centre of the simulation volume, while the second simulation started from unconstrained initial conditions. We will refer to the first simulation as the ‘cluster model’, and to the second one as the ‘field model’.

The importance of overmerging is most clearly illustrated by looking at cumulative dark halo mass functions

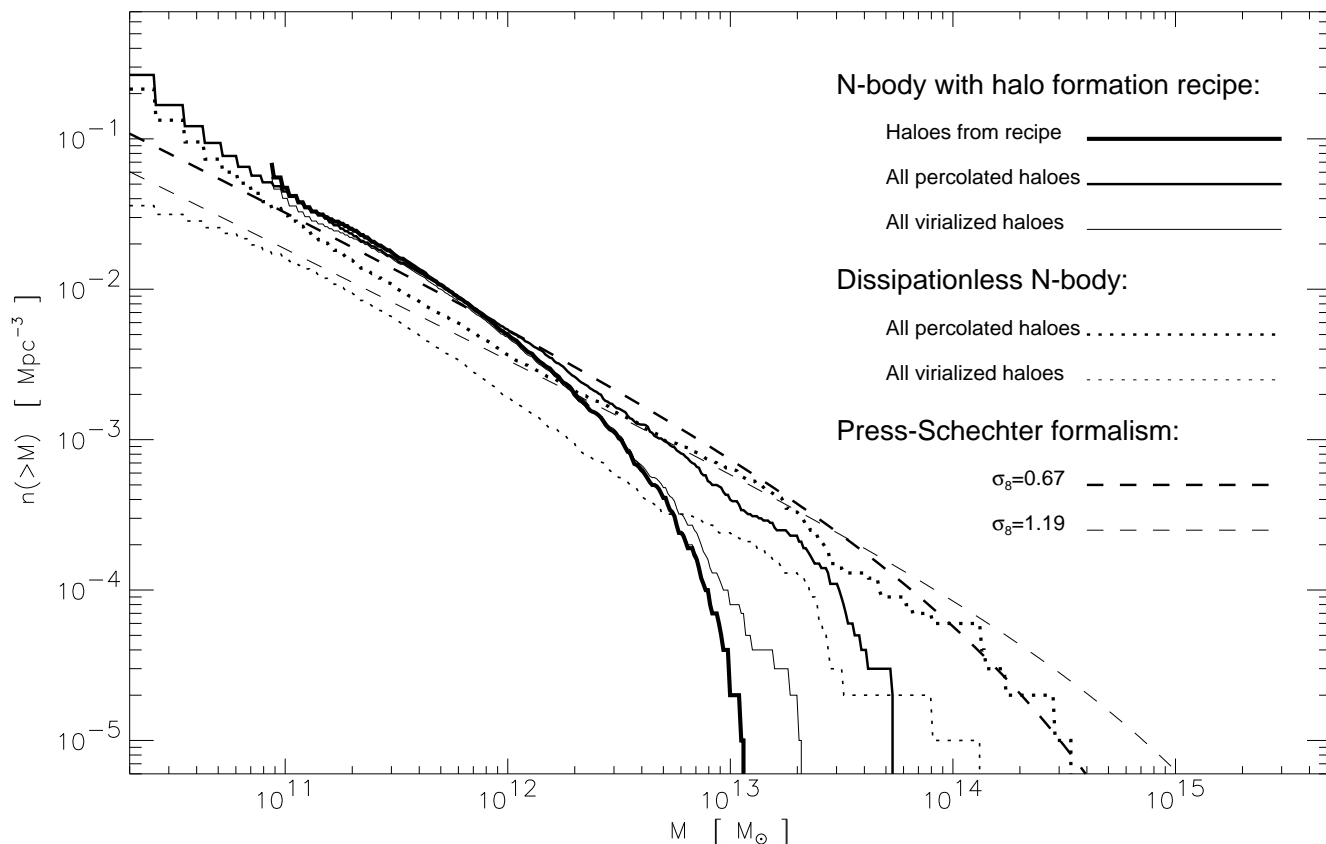


Figure 2. A comparison of galaxy halo cumulative mass distributions. Dashed lines show the mass function for the Press-Schechter formalism for standard CDM with two different normalizations: $\sigma_8 = 0.67$ (thick dashed line), and the COBE normalization ($\sigma_8 = 1.19$, thin dashed line). The thick dotted line represents the mass function for all haloes identified in a standard dissipationless N-body simulation (for $\sigma_8 = 0.67$) using the percolation algorithm, while the thin dotted line shows the subset of those haloes that have virialized. The thickest solid line shows the mass functions for haloes formed using the recipe of van Kampen (1995, 1997), starting from the same initial conditions. Including all haloes found from the percolation algorithm time at the final time results in the mass function depicted by the thinnest solid line, while the solid line with intermediate thickness shows the subset of these haloes that have virialized. Note the difference between the thin solid line and the thin dotted line, which were obtained using the same group finder.

as produced by the Press-Schechter formalism, a standard N-body simulation, and the present method, as described above.

In Fig. 2 we compare all these to each other. The thick dashed line is the halo function from the Press-Schechter formalism for the cosmology adopted here, with $\sigma_8 = 0.62$. The COBE normalized version (i.e. $\sigma_8 = 1.19$) is also shown, as a thin dashed line. We ran the field model without the galaxy halo formation recipe switched on, i.e. just as a traditional N-body simulation, and obtained the mass function using the same group finder (see Section 3.3.3) used in the full simulation technique. This mass function is plotted in Fig. 2 as a thick dotted line. It clearly matches the Press-Schechter mass function. However, if we now plot the mass function for *virialized haloes only*, being haloes which satisfy eq. (1) within 25 per cent, it falls short by a factor of two (thin dotted line). This is because in the EPS formalism all collapsed haloes are assumed to virialize, while haloes as identified in numerical simulations change through merging, secondary infall, tidal forces, etc., and are therefore not able to remain virialized at all times. This is even true for

galaxy cluster haloes (Natarajan, Hjorth & van Kampen 1997). Thus, virialized haloes form a subset of all haloes at any one time. Indeed, the haloes formed in our simulations contain about 25 per cent of all the mass in the universe, while in the EPS formalism all matter is contained in haloes, by design.

The halo functions that are produced by the full simulations are shown in Fig. 2 as solid lines. The thickest of the three lines represents the halo function for the galaxy haloes identified by the recipe. The thinnest solid line shows the effect of adding the virialized haloes identified at $z = 0$, including the ones above the upper mass-limit. Note that there are only a few more haloes added, so our upper mass-limit for halo particles is close to the maximum mass found from the halo formation recipe employed.

The right-most solid line shows the mass function for all percolated systems at $z = 0$: galaxy halo particles, newly virialized haloes, and all other collapsed haloes. We see that locking matter in haloes at early times has the effect that the largest mass haloes that form in both the Press-Schechter formalism and standard N-body simulations are

now correctly resolved into subhaloes and are not counted as single objects. More interestingly, the maximum mass found for virialized haloes is close to that found for observed galaxies. The core of the simulated cluster is one of these most massive virialized haloes.

Because of our choice for the upper-limit to halo particles, the most massive haloes are not treated as single particles. However, they are identified in the simulation, and are incorporated into the merger tree used for the phenomenological galaxy formation model.

4 RESOLVING THE TULLY-FISHER / LUMINOSITY FUNCTION DISCREPANCY

Before showing our model results, a word of warning: throughout this section we plot Tully-Fisher diagrams that contain *all* model galaxies found from the modelling. We should therefore bear in mind that only a subset of all these galaxies, i.e. the spirals, actually belong in such a diagram. As we do not model the morphologies of the galaxies, we aim to at least cover the region of $V_c - M_I$ space occupied by the observational data. Galaxies outside that region may in fact be regarded as ellipticals, S0's, and irregular galaxies, and their properties should be tested using other observational relations, like the Faber-Jackson relation, which is the analogue of the Tully-Fisher relation for ellipticals.

One could be tempted to merge the Tully-Fisher and Faber-Jackson relations into one diagram, as the circular velocity is related to the velocity dispersion through the assumption of an isothermal density profile. However, the Faber-Jackson relation concerns the *central* velocity dispersion, which is not equal to, and usually larger than, the velocity dispersion of the dark matter halo. White (1979) found that merger remnants tend towards a r^{-3} density profile, so if elliptical form through merging, they should have declining circular velocity profiles. Observationally, it is very difficult to measure halo properties of generally gas-poor elliptical galaxies, whereas spiral galaxies have sufficient cold gas at large radii to act as a tracer of the halo potential. Thus, we need more detailed modelling before we can attempt a match to the Faber-Jackson relation, and we therefore restrict ourselves to the Tully-Fisher relation for now.

4.1 Repeating CAFNZ: model m

To see the effect of using a merger tree obtained from numerical simulations that employ the halo formation recipe of van Kampen (1997), instead of a merger tree generated according to the extended Press-Schechter formalism, we applied the same prescription of gas dynamics and star formation that CAFNZ used, with the same parameters ($\tau_*^0 = 2$ Gyr etc.). The only other difference with the CAFNZ model beside the halo population is the choice of IMF and stellar population models (see Table 1), but we believe these differences to be marginal (see Appendix A). The spherical infall model has been adopted to calculate the circular velocity, as in CAFNZ.

The result for the cluster simulation is plotted in Fig. 3a. What is apparent from this figure is that we reproduce the CAFNZ Tully-Fisher relation, but miss the high- V_c end of it. Because our model galaxy haloes do not overmerge, the large- V_c haloes found by CAFNZ are divided into a number

of smaller haloes in our modelling (see Section 3.3). The effect on the B and K band luminosity function is a shift to the fainter end, as is shown in Fig. 4a. The thick line is the luminosity function found by CAFNZ, while the symbols with error bars represent the observational data described above. Our model m results quite clearly fit neither the observations nor the CAFNZ models. But this is actually a very nice result, as it allows us to resolve much of the Tully-Fisher / luminosity function discrepancy, as follows.

4.2 Setting $\Upsilon = 1$: model n

Considering the ‘brakes’ that CAFNZ had to apply to their models, it should come as a relief that our model galaxies are too faint in B and K, since the I-band magnitudes were already too faint for the Tully-Fisher relation to fit. We can thus apply an *overall brightening* to the modelling in order to simultaneously match the Tully-Fisher relation and both luminosity functions. This is easily achieved by setting $\Upsilon = 1$ instead of $\Upsilon = 2.7$, which was the value that CAFNZ needed to adopt. This brightens the I-band Tully-Fisher relation by just over a magnitude, with the result that the predicted distribution of points now overlaps with the observational data (Fig. 3b). If we assume that the brightest galaxies in I (for a given V_c) are those that were still forming stars up to a fairly recent epoch, and are therefore likely to be spirals, the predicted Tully-Fisher relation can be considered encouraging, except for the faint end. We discuss solutions to that at the end of this Section.

The luminosity functions are shown in Fig. 4b, in the corresponding panel. The luminosity function matches the observations very well in the B-band, but falls short in the K-band. In the next section we therefore introduce two more ingredients that not only render the modelling more realistic, but provides a better to the K-band luminosity function: chemical evolution and starbursts.

5 CHEMICAL EVOLUTION AND STARBURSTS

5.1 Adding chemical evolution: model c

Instead of adopting primordial metallicity for the cooling function, and constant solar metallicity for the stellar populations, we now incorporate a chemical evolution model. The details of the method we use is described in Appendix C. This means that we use a different set of stellar population models, with evolving metallicities. Once a population forms, the *initial* metallicity and the star formation timescale τ_* determines what the metallicity will be at later times. The enrichment of hot gas by chemically evolving stellar populations will increase the number of stars forming at later times, because the cooling function depends on the metallicity. We assume enrichment to be efficient, i.e. the metallicity of the cooling gas is equal to that of the populations it cools to (mass-averaged over co-existing populations in merged galaxies).

The effect on the Tully-Fisher relation of the inclusion of chemical evolution can be seen in Fig. 3c, whereas the effect on the luminosity functions is shown in Fig. 4c. We see that the B-band luminosity function ends up too bright, whereas the K-band one is still too faint. In other words,

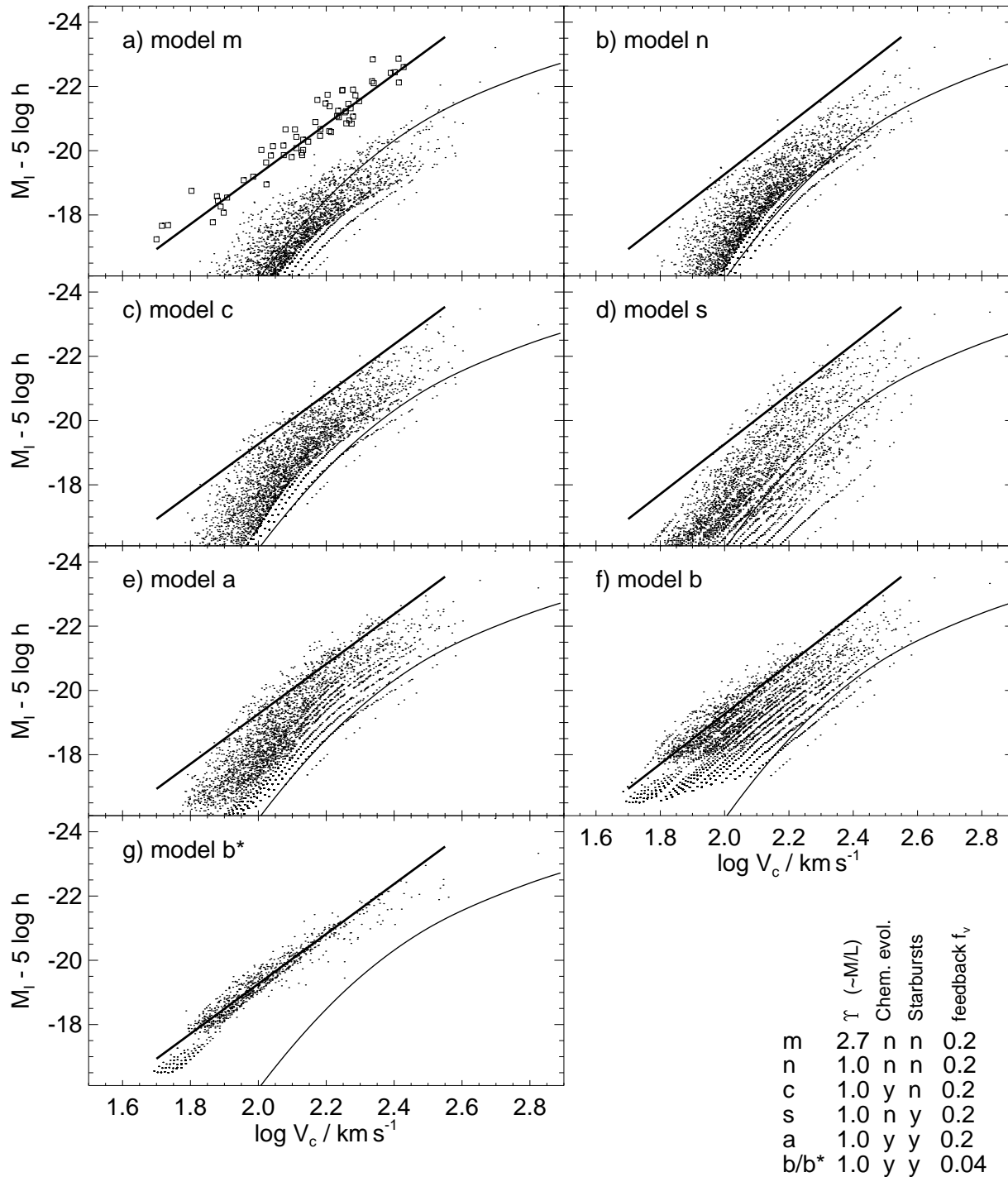


Figure 3. I-band Tully-Fisher relation from our modelling (dots) for various choices of parameters. The first six panels correspond to the six models discussed in the text, whereas the bottom left panel shows model b for a subset of the data that should represent an observational dataset (see Section 3.4.6 for details). We refer to the legenda and to Table 1 for the exact model specifications. Also shown are fits to the distributions from CAFNZ (curved thin solid line), observational data averaged over four different sets of data (straight thick solid line, see main text for details). In the top left panel we added observational data by Tully et al. (1998), shown as squares. Note that the specific redshifts at which the galaxy formation recipe is applied are clearly visible for model b, and to a lesser extent for the other models, due to the simplified modelling of starbursts.

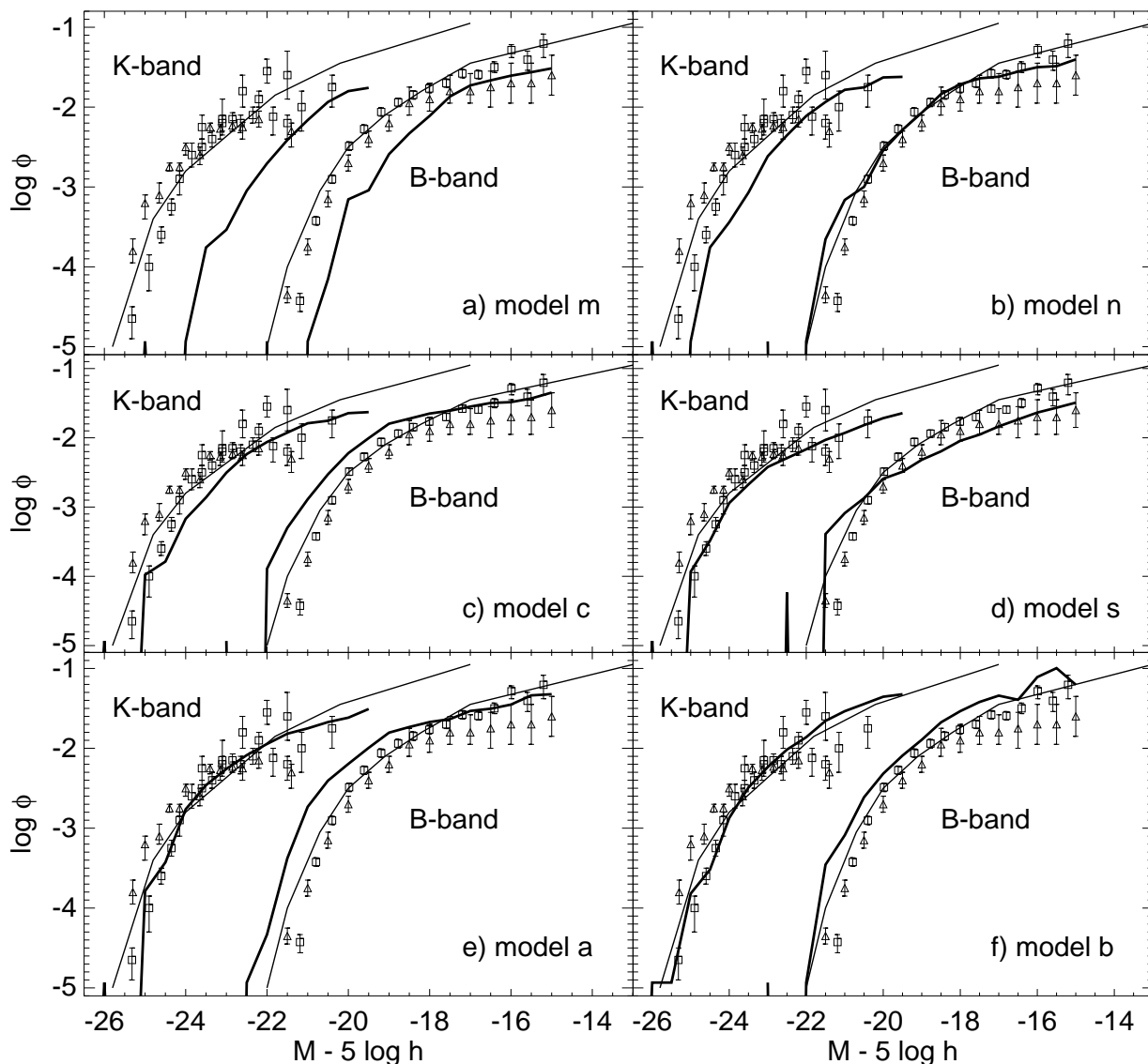


Figure 4. B and K band luminosity functions from our modelling (thick solid lines), corresponding to the Tully-Fisher relations shown in Fig. 5 (in the same order), and those from CAFNZ (thin solid lines). Please refer to the legenda of Fig. 3 and Table 1 for details on the models. Also shown are old observational data (triangles) from Loveday et al. (1992) for the B-band and Mobasher et al. (1993) for the K-band, and new observational data (squares) from Zucca et al. (1997) for the B-band and Gardner et al. (1997) and Glazebrook et al. (1995) for the K-band.

most galaxies end up too blue. The reason for this is that chemical enrichment boosts late stars formation with relatively slowly decaying star formation rates. This means that we have to find a way to form stars earlier and with much more rapidly decaying star formation rates. This leads us to the conclusion that we need to incorporate a bursting mode of star formation, driven by merging activity, which is most significant at early times (e.g. Carlberg 1990).

Another possibility is the addition of a dust model, which will typically render galaxies redder. However, we leave this for future work to explore.

5.2 Models with starbursts only: model s

In order to see the effect of adding a bursting mode of star formation, we first look at a burst-only model in which continuous galaxy formation is effectively switched off. We make the burst as strong as possible, with f_b set to a very large value, and with a very short decay-time. However, the duration of the starburst is set as described in Appendix B.

The Tully-Fisher relation produced by this pure starburst model is shown Fig. 3d. It is quite similar to the chemical evolution model, in the sense that more stars are formed, which brings enough galaxies on or towards the Tully-Fisher relation. The spread is a bit larger, as the earliest galaxies

fade more rapidly if they experience just a single starburst, therefore ending up fainter than in model c, whereas the late mergers are brighter because more gas is used up at the present epoch than in model c, which has a much larger star formation time-scale.

However, the luminosity functions, as shown in Fig. 4d, are different from the chemical evolution ones in the sense that the colours end up much redder, providing a better match to the observational data for both bands.

5.3 Models with both chemical evolution and starbursts: models a and b

The pure starburst model produces fairly monochromatic galaxies: all galaxies redden quickly and effectively stop forming stars, because most mergers happen at high redshifts (e.g. Carlberg 1990), with a merger rate peak at $z \approx 1$ (van Kampen 1997). If we now switch on continuous galaxy formation again, those galaxies that have some gas left (likely to be spirals), can form a (cosmologically) young blue population that broadens the colour distribution *and* moves those galaxies on top of the observed Tully-Fisher relation. After all, this relation is based on spiral galaxies in which some star formation activity is typically found. In order to achieve this we set $f_b = 100$ and $\tau_{*,b}^0 = 0.01$ Gyr.

The resulting Tully-Fisher relation is plotted in Fig. 3e, and the luminosity functions in Fig. 4e. They all match the observational data reasonably well, except for the faint end of the Tully-Fisher relation. However, we can easily ‘lift’ this faint end by decreasing the amount of feedback to $f_v = 0.04$, which comprises model b. The resulting Tully-Fisher relation is plotted in Fig. 3f, and this is clearly shown to work. It slightly improves the B-band luminosity function at the bright end, but at the same time worsens it at the faint end, as shown in Figs. 4f.

Finally, note that the remaining deviations from the observed luminosity functions are likely to be resolved by taking into account dust, which will redden the colours of the galaxies.

5.3.1 Observational selection

So far we have made no attempt at discriminating between the model galaxies, which makes quite a difference for the Tully-Fisher relation, as only spiral galaxies enter the relation, and only those for which a reliable circular velocity can be measured. This means that spiral galaxies showing any sign of interaction are typically excluded from an observational sample. Thus, we should disregard any model galaxy that underwent a major merging event within the last 1-2 Gyr. Furthermore, galaxies that have not been part of a major merger event for a long time, will have a much reduced star formation rate, and are therefore not likely to possess an obvious disk component. So we should also disregard galaxies that have formed at fairly high redshift and evolved passively up to the present epoch.

We select an ‘observational Tully-Fisher sample’ from all model galaxies by selecting only those galaxies that satisfy $1 \text{ Gyr} < t_{\text{last}} < 6 \text{ Gyr}$, where t_{last} is the look-back time for the last major merging (or formation) event. This corresponds to (approximately) a redshift range of $0.05 < z_{\text{last}} < 0.5$. These are plotted in Fig. 3g. Clearly,

this subset of the model data provides a reasonable match to the observational Tully-Fisher data. However, this attempt at observational selection is rather crude, and will need to be refined in future work. A proper disk model is a necessity, as is a dust model which takes the inclination of the disk into account.

6 DISCUSSION AND CONCLUSIONS

We have argued that overmerging is an important problem for phenomenological galaxy formation models, and is largely responsible for the discrepancy found in earlier work between the Tully-Fisher relation and the luminosity function. We resolved the overmerging problem by using an N-body simulation technique that includes a galaxy halo formation recipe. We combined this technique with simplified gas dynamics and star formation physics, and a recent stellar population model, in order to phenomenologically describe galaxy formation and evolution. We included chemical evolution, and two modes of star formation: major bursts of star formation, and a quiescent mode in which stars form more continuously.

With this set-up we match both the B and K band luminosity function and the I-band Tully-Fisher relation, for an $\Omega = 1$ standard CDM structure formation scenario. Resolving the overmerging problem is the major contributor to this result, but the inclusion of chemical evolution and starbursts are also important ingredients.

The new ingredients we have added to the modelling of galaxy formation are needed in order to make the models more realistic, and are not introduced simply in order to give yet more free parameters. Nevertheless, our resolution to the Tully-Fisher / luminosity function discrepancy may well not be unique, and various other changes to the ingredients of the phenomenological galaxy formation recipe might produce similar results. For example, we have not studied the influence cosmological parameters have on the model galaxy populations, where Ω , Λ , and σ_8 are likely to be the important parameters. Other types of ingredients are possible as well: Somerville & Primack (1998) resolve some of the discrepancy using a dust extinction model plus a halo-disk approach to feedback.

We intend to explore these issues in future work. One way of resolving the worries about degeneracies in the cosmological/physical parameter space will be to include data at intermediate and high redshifts. Nevertheless, although the present work has concentrated on modelling the properties of the low-redshift universe only, we believe that the issues we have raised are sufficiently general that they will invariably be part of any successful model for galaxy formation.

ACKNOWLEDGEMENTS

We thank the anonymous referee for a report that encouraged us to clarify some parts of this paper, and Carlton Baugh, Shaun Cole, and Eduard Thommes for useful comments.

REFERENCES

Barnes J.E., Hut P., 1986, *Nat*, 324, 446

Binney J., 1977, *ApJ*, 215, 483
 Bond J.R., Cole S., Efstathiou G., Kaiser N., 1991, *ApJ*, 379, 440
 Bower R.J., 1991, *MNRAS*, 248, 332
 Carlberg R.G., 1990, *ApJ*, 350, 505
 Carlberg R.G., 1994, *ApJ*, 433, 468
 Cole S., Aragón-Salamanca A., Frenk C.S., Navarro J.F., Zepf S.E., 1994, *MNRAS*, 271, 781
 Davis M., Efstathiou G., Frenk C.S., White S.D.M., 1985, *ApJ*, 292, 371
 Efstathiou G., Frenk C.S., White S.D.M., Davis M., 1988, *MNRAS*, 235, 715
 Elmegreen B., 1999, in Beckman J., ed., *Formation and evolution of galaxies on cosmological timescales*, Cambridge University Press
 Faber S.M., Gallagher J.S., 1979, *ARAA*, 17, 135
 Gardner J.P., Sharples R.M., Frenk C.S., Carrasco B.E., 1997, *ApJ*, 480, 99
 Giovanelli R., Haynes M.P., da Costa L.N., Freudling W., Salzer J.J., Wegner G., *ApJ*, 477, L1
 Glazebrook K., Peacock J.A., Miller L., Collins C., 1995, *MNRAS*, 275, 169
 Heavens A.F., Jimenez R., 1999, submitted to *MNRAS*
 Heyl J.S., Cole S., Frenk C.S., Navarro J.F., 1995, *MNRAS*, 274, 755
 Jimenez R., Padoan P., Matteucci F., Heavens A., 1998, *MNRAS*, 299, 123
 Jimenez R., Dunlop J., Peacock J., MacDonald J., Jørgenson U.G., 1999, *MNRAS*, in press
 Kauffman G., White S.D.M., 1993, *MNRAS*, 261, 921
 Kauffman G., White S.D.M., Guiderdoni, 1993, *MNRAS*, 264, 201
 Kauffman G., Colberg J.M., Diaferio A., White S.D.M., 1998, *astro-ph/9805283*
 Klypin A., Gottlöber S., Kravtsov A.V., 1997, *astro-ph/9708191*
 Kurucz R., 1992, *ATLAS9 Stellar Atmosphere Programs and 2 km/s Grid CDROM Vol. 13*
 Lacey C.G., Cole S., 1993, *MNRAS*, 262, 627
 Longair M.S., 1998, *Galaxy formation*, Springer Verlag
 Loveday J., Peterson B.A., Efstathiou G., Maddox S.J., 1992, *ApJ*, 90, 338
 Mathewson D.S., Ford V.L., Buchhorn M., 1992, *ApJS*, 81, 413
 Matteucci F., Francois P., 1989, *MNRAS*, 239, 885
 Mihos J.C., Hernquist L., 1994, *ApJ*, 431, L9
 Mihos J.C., Hernquist L., 1996, *ApJ*, 464, 641
 Mobasher B., Ellis R.S., Sharples R.M., 1986, *MNRAS*, 223, 11
 Moore B., Governato F., Quinn T., Stadel J., Lake G., 1998, *ApJ*, 499, L5
 Mould J.R., Akeson R.L., Bothun G.D., Han M-S., Huchra J.P., Roth J., Schommer R.A., 1993, *ApJ*, 409, 14
 Natarajan P., Hjorth J., van Kampen E., 1997, *MNRAS*, 286, 329
 Navarro J.F., White S.D.M., 1993, *MNRAS*, 265, 271
 Peebles P.J.M., 1980, *Large-scale structure in the Universe*, Princeton
 Pierce M.J., Tully R.B., 1992, *ApJ*, 387, 47
 Press W.H., Schechter P., 1974, *ApJ*, 187, 425
 Rees M.J., Ostriker J.P., 1977, *MNRAS*, 179, 541
 Roberts M.S., Haynes M.P., 1994, *ARAA*, 32, 115
 Sanders D.B., Mirabel I.F., 1996, *ARAA*, 34, 749
 Silk J., 1977, *ApJ*, 211, 638
 Somerville R.S., Lemson G., Kolatt T.S., Dekel A., 1998, *astro-ph/9807277*
 Somerville R.S., Primack J.R., 1998, *astro-ph/9802268*
 Spitzer Jr. L., 1969, *ApJ*, 158, L139
 Sugimotohara T., Suto Y., 1992, *ApJ*, 396, 395
 Sutherland R., Dopita M.A., 1993, *ApJS*, 88, 253
 Tormen G., Diaferio A., Syer D., 1998, 299, 728

Tully R.B., Pierce M., Huang J.-S., Saunders W., Verheijen M., Witchalls P., 1998, *AJ*, 115, 2264
 van Kampen E., 1995, *MNRAS*, 273, 295
 van Kampen E., 1997, in Clarke D.A., West M.J., eds., *Proc. 12th 'Kingston meeting' on Theoretical Astrophysics: Computational Astrophysics*, ASP Conf. Ser. Vol. 123. Astron. Soc. Pac., San Francisco, p. 231, *astro-ph/9904270*
 White S.D.M., 1976, *MNRAS*, 177, 717
 White S.D.M., 1979, *MNRAS*, 189, 831
 White S.D.M., 1996, in Schaeffer et al., eds., *Cosmology and Large-scale structure*, Proc. 60th Les Houches School, Elsevier, p.349
 Zucca E., Zamorani G., Vettolani G., Cappi A.S., Merighi R., Mignoli M., Stirpe G.M., MacGillivray H., et al., 1997, *A&A*, 326, 477

APPENDIX A: DETAILS OF THE GALAXY FORMATION RECIPE

This Appendix provides some further details of the phenomenological modelling of galaxy formation adopted for this paper. We chose to use the modelling of CAFNZ as a starting point, but note that many authors use similar models with differences in the details or in the choice of parameters. Significant changes to the CAFNZ models are: the halo merger history and mass function, the inclusion of star bursts, and the modelling of chemical evolution. All parameters encountered in the various ingredients of the model are listed in Table 1, along with their values for the specific models discussed in the main paper.

HALO POPULATION AND ITS MERGER HISTORY

In most phenomenological galaxy formation recipes published so far the galaxy halo population and its formation and merger history are obtained from the extended Press-Schechter (EPS) model (see the introduction for references). Instead, we use the haloes found in N-body simulations which includes a recipe for the formation of galaxy haloes (van Kampen 1995, 1997), as described in Section 3.3.3. The actual N-body code used is the Barnes & Hut (1986) treecode.

Haloes are assumed to form according to the spherical collapse model (e.g. Peebles 1980), and are assumed to settle as isothermal spheres, with a constant circular velocity V_c . The spherical collapse model provides a relation between the mass of the halo, its circular velocity, and its formation redshift (e.g. White 1996) :

$$V_c = \left(\frac{M_{\text{halo}}}{2.35 \times 10^5 h^{-1} M_\odot} \right)^{\frac{1}{3}} \left(1 + z_{\text{form}} \right)^{\frac{1}{2}} \text{ kms}^{-1}, \quad (\text{A1})$$

where a truncated isothermal density profile has been assumed. One is forced to adopt this crude model as the extended Press-Schechter formalism that is typically used does not provide information on the kinematics of the haloes. The N-body simulations do provide us with that information, so we can obtain V_c directly from the velocity dispersion of the halo, which is in virial equilibrium by definition. Again assuming an isothermal density profile, we have

$$V_c = \left(\frac{2}{3} \right)^{\frac{1}{2}} \langle v^2 \rangle^{\frac{1}{2}} \approx \left(0.33 \frac{GM_{\text{halo}}}{R_h} \right)^{\frac{1}{2}}, \quad (\text{A2})$$

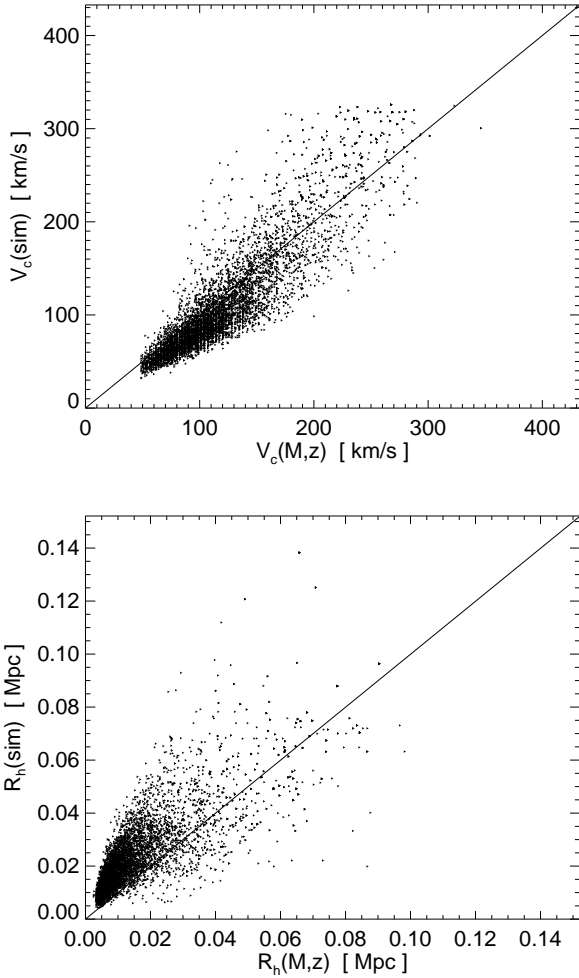


Figure A1. Comparison of circular velocity from the spherical infall model and from N-body simulations (top panel), and a similar comparison for the half-mass radii (bottom panel). The solid lines simply indicate equality.

where $\langle v^2 \rangle$ is obtained from the numerical simulation. Basically, we allow dark haloes with the same mass and z_{form} to have a range of values for R_h , and therefore different V_c , while CAFNZ assume the fixed value

$$\left(\frac{R_h}{100h^{-1}\text{kpc}} \right) = \left(\frac{M_{\text{halo}}}{6.37 \times 10^{12}h^{-1}M_{\odot}} \right)^{\frac{1}{3}} \frac{1}{1 + z_{\text{form}}}. \quad (\text{A3})$$

In order to access the significance of the difference between using $V_c(\langle v^2 \rangle)$ and $V_c(M, z)$, we plotted $V_c(M, z)$ versus $V_c(\langle v^2 \rangle)$ (Fig. A1). Clearly, on *average* the spherical infall model is a good approximation. The scatter represents the spread in half-mass radii and velocity dispersions for a given mass found in the simulations. An upper limit to the mass of a galaxy halo particle needs to be set, as discussed in detail in Section 3.3.4.

In practice, we set the upper mass limit to be $7 \times 10^{13}h^{-1}M_{\odot}$, or about 1600 of the initial simulation particles. Although justifiable in numerical terms, this mass is also close to the one that results from the cooling criterion $t_{\text{cool}} < t_{\text{coll}}$, where t_{coll} is the halo collapse time for the spherical collapse model (Rees & Ostriker 1977; Binney

1977; Silk 1977). For primordial abundances, this limit is about $1.5 \times 10^{13}\Omega_b h^{-1}M_{\odot}$ (White 1996), i.e. $\approx 1.0h^{-1} \times 10^{12}M_{\odot}$ for our choice of Ω_b . For enriched gas, with abundances near solar, the limit goes up to $5 - 10 \times 10^{13}h^{-1}M_{\odot}$.

FORMATION AND MERGING OF GALAXIES WITHIN DARK HALOES

For the modelling of the galaxies that populate the dark matter haloes we follow the approach of CAFNZ. In their scheme, galaxies form in the centre of dark haloes. When dark haloes merge, their galaxies merge with a delay giving by the dynamical friction timescale. During this dynamical friction phase a dark halo can thus contain several galaxies at the same time. One of these galaxies will be designated as the galaxy to which halo hot gas can cool, while the others are considered satellites. It is important to realize that this part of the CAFNZ prescription is kept identical, whereas the formation and evolution of the dark halo population is different. Thus, dynamical friction is assumed to delay the merging of galaxies within merged haloes, with the delay given by

$$\tau_{\text{mrg}} = \tau_{\text{mrg}}^0 (M_{\text{halo}}/M_{\text{gal}})^{\alpha_{\text{mrg}}}. \quad (\text{A4})$$

In the following, all gas dynamics and star formation happens in between ‘major events’, which are either the formation of a halo (plus galaxy), the merger of one or more haloes, or the merger of one or more galaxies within an already merged halo. These three events define lifetimes for haloes and galaxies over which gas can cool, stars can form, etc., according to processes we describe next.

STARS AND GAS

Gas dynamics and star formation are modelled using analytical relations that are power-law functions of the halo circular velocity, V_c , which is a constant for a given halo as we assume an isothermal density profile.

Each galaxy has a reservoir of stars, cold gas, and hot gas. A newly formed galaxy has all its baryons, with a total mass of $\Omega_b M_{\text{halo}}$, in the form of hot gas. The gas temperature is assumed to quickly settle to the virial temperature, which is a function of V_c only:

$$T_{\text{gas}} = T_{\text{vir}} = \frac{\mu m_p}{2k} V_c^2. \quad (\text{A5})$$

The three constants μ , m_p and k are the mean molecular weight, proton mass, and Boltzmann’s constant, respectively. Hot gas will cool radiatively at a rate which depends on the density ρ , temperature T , and metallicity Z of the hot gas. The cooling time-scale is given by

$$\tau_{\text{cool}} = \frac{3}{2} \frac{\rho_{\text{gas}}(r)}{\mu m_p} \frac{kT_{\text{gas}}}{n_e^2(r)\Lambda(T_{\text{gas}}, Z_{\text{gas}})}, \quad (\text{A6})$$

where n_e is the electron density, and $\Lambda(T, Z)$ the cooling function. For the latter we take the cooling functions for primordial and solar metallicities as given by Sutherland & Dopita (1993), and obtain the cooling function for any given metallicity by linear interpolation or extrapolation of $\log \Lambda(T, 0.0002)$ and $\log \Lambda(T, Z_{\odot})$.

For gas at a constant temperature with a homogeneous chemical abundance, the cooling rate depends only on the density, and is therefore a function of radius. Thus, at a

large enough radius r_{cool} the cooling time will be larger than the time passed between two major halo events (formation or merger). The mass encompassed by this cooling radius is transferred from the hot to the cold gas reservoir between these two events.

Stars can form from cold gas, thus transferring mass from the cold gas reservoir to the stellar population of the galaxy. In the present modelling, mass ejected by dying stars is *not* transferred back to any of the gas reservoirs. However, cold gas can be reheated and thus transferred back to the hot gas reservoir by the energy output of supernovae. This process is called ‘feedback’ for short.

The star formation rate is proportional to the amount of cold gas actually available:

$$dM_*(t, V_c)/dt = M_{\text{cold}}(t, V_c)/\tau_*(V_c), \quad (\text{A7})$$

with the star formation time-scale given by

$$\tau_*(V_c) = \tau_*^0 (V_c/300 \text{ km s}^{-1})^{\alpha_*}. \quad (\text{A8})$$

It is assumed that the reheating of cold gas by supernovae can be modelled as

$$dM_{\text{hot}}(t, V_c)/dt = \beta(V_c) dM_*(t, V_c)/dt, \quad (\text{A9})$$

where the feedback proportionality parameter β is given by

$$\beta(V_c) = (V_c/V_{\text{hot}})^{-\alpha_{\text{hot}}}. \quad (\text{A10})$$

The overall feedback parameter f_v , defined as the fraction of energy released by supernovae that is dumped into the cold gas reservoir as kinetic energy, determines the values of the constants α_* , α_{hot} , and V_{hot} . In this paper we mostly use $f_v = 0.2$, for which CAFNZ found the following values from fits to simulation data by Navarro & White (1993): $\alpha_* = -1.5$, $\alpha_{\text{hot}} = 5.5$, and $V_{\text{hot}} = 140 \text{ km s}^{-1}$. For a detailed description of the feedback process and its parameters we refer to CAFNZ.

The merging of haloes and galaxies also determine where stars, cold, and hot gas end up. A merger of haloes brings together all amounts of hot gas of the merging haloes, and reheat the new single hot gas reservoir to the virial temperature of the newly formed halo. It also brings together all galaxies that were part of the original haloes. The most massive of these will now be the one to which hot gas can cool and form stars. CAFNZ set the circular velocity of this halo to be that of the newly formed dark halo, which can be rather large, unless its merger time τ_{mrg} , as given by eq. (A4), is larger than the time available until the next merger event (or the present epoch), in which case the original V_c is retained.

All other galaxies retain their identity (their stars and cold gas reservoir) if they do not merge with the most massive one, i.e. if τ_{mrg} is smaller than the time available until the next merger event (or the present epoch). In that case stars keep forming from the cold gas left in each of those galaxies, whereas feedback not only reheats part of the gas, but also expells it to the hot gas reservoir of the common dark halo.

STELLAR POPULATION MODELS

To predict the spectra and photometric properties of galaxies we have used the extensive library of synthetic stellar population models computed by Jimenez et al. (1998; 1999),

where a detailed description of the models can be found. Here we briefly review the main ingredients of the models. We computed simple synthetic stellar populations (SSPs), i.e. stellar populations with fixed metallicity and formed in a burst of infinitesimal duration, for metallicities between $1/100 Z_{\odot}$ and $2 Z_{\odot}$ and ages between 0.01 and 14 Gyr. The library uses new interior models (Jimenez et al. 1998) and a new set of stellar photospheres for the coolest models ($T_{\text{eff}} < 6000$), while Kurucz (1992) models are used for $T_{\text{eff}} > 6000\text{K}$. Two important new features of the models are the inclusion of an accurate treatment of all post-main sequence evolutionary stages and the use of better theoretical photospheric models for low temperatures.

Simple stellar populations (SSP’s) are the building blocks of any arbitrarily complicated population since the latter can be computed as a sum of SSP’s, once the star formation rate is provided. In other words, the luminosity of a stellar population of age t_0 (since the beginning of star formation) can be written as:

$$L_{\lambda}(t_0) = \int_0^{t_0} \int_{Z_i}^{Z_f} L_{\lambda}^{\text{SSP}}(Z, t_0 - t) dZ dt \quad (\text{A11})$$

where the luminosity of the SSP is:

$$L_{\lambda}^{\text{SSP}}(Z, t_0 - t) = \int_{m_d}^{m_u} \dot{M}_*(Z, m, t) l_{\lambda}(Z, m, t_0 - t) dm \quad (\text{A12})$$

and $l_{\lambda}(Z, m, t_0 - t)$ is the luminosity of a star of mass m , metallicity Z and age $t_0 - t$, Z_i and Z_f are the initial and final metallicities, m_d and m_u are the smallest and largest stellar mass in the population and $dM_*(Z, m, t)/dt$ is the star formation rate at the time t when the SSP is formed.

We assume that the initial mass function (IMF) is universal and is given by a Salpeter IMF ($x = 1.35$). In order to take account for the chemical evolution we have computed detailed models that link dM_*/dt and Z , i.e. $M_*(Z, t)$ since we have assumed that the m dependence is constant (a constant IMF). This is described in Appendix C.

APPENDIX B: STARBURSTS

Besides a quiescent mode of star formation, we consider a bursting mode of star formation associated with a major formation or merging event. This star formation mode can be the dominant one, especially at early times when encounters and mergers are frequent, and most galaxies form. The strength of the starburst will depend on the clumpiness of the matter distribution that is induced by an encounter or merging event, on the duration of the starburst phase, and on the amount of cold gas available to form stars, which can be substantially enhanced by strong inflows of gas into the central region of the galaxy during the final stages of a merger event (Mihos & Hernquist 1996). Here we adopt a simplified approach, by assuming that the SFR during the starburst phase can be modelled using the same scaling relations as for the quiescent star formation mode, but with different star formation and cooling rates. The feedback strength is assumed to be the same for both star formation modes. Also, we adopt the same Salpeter IMF for both modes, a choice that is supported by recent observational data (see Elmegreen 1999).

The duration of the starburst, t_b , is assumed to be equal to the dynamical timescale of the new dark matter halo:

$t_b = \tau_{\text{dyn}} \equiv R_h/\sigma_v$. Using the spherical infall model (eq. A1), the virial theorem (eq. 1), and the isothermal profile (eq. A2), we find

$$t_b \approx 0.024(1 + z_{\text{form}})^{-3/2} h^{-1} \text{Gyr}. \quad (B1)$$

Therefore, a single starburst at low redshift lasts longer than one at high redshift, but as the frequency is much lower, it will still be at high redshifts that starbursts are more important. Note that the actual starburst might last for a much shorter time than the dynamical timescale, depending on the amount of material available in the bulges of the merging galaxies (Mihos & Hernquist 1994), so t_b should be taken as a maximum.

The bursting star formation timescale $\tau_{*,b}$ is assumed to scale with the halo circular velocity V_c in the same manner as the continuous star formation timescale τ_* , i.e.

$$\tau_{*,b}(V_c) = \tau_{*,b}^0 (V_c/300 \text{ km s}^{-1})^{\alpha_*} \quad (B2)$$

(analogous to eq. (A8) in Appendix A).

It is also necessary to introduce a ‘burst factor’ f_b which models the enhanced cooling of hot gas and stronger inflow of cold gas during the star bursting phase. It is expressed as a density enhancement over and above the mean isothermal profile that will form after the bursting event. If f_b is larger than unity, cooling will be more efficient, so that star formation will be enhanced during the bursting phase.

Thus, during a starburst of duration t_b , star formation is enhanced by having more cold gas available to form stars, and by having those stars formed at a higher rate. The shorter star formation timescale will result in a different stellar population as compared to the continuous mode for two reasons: firstly and simply due to the different formation timescale, but secondly because the chemical evolution of the population will be different.

APPENDIX C: CHEMICAL EVOLUTION

Most of the phenomenological models published so far make the simplifying assumption that hot gas cools with primordial metallicity, while the stellar populations form and evolve at a constant solar metallicity. This ‘instant’ enrichment scheme helps to produce galaxies that are red enough in order to match observations, but is only realistic for star bursting galaxies, not for galaxies that form stars more continuously. Furthermore, the hot gas around metal-ejecting galaxies is enriched, which will boost cooling at intermediate and low redshifts. We therefore include chemical enrichment in our modelling, in the following way.

The chemical evolution of a stellar population can be divided into two parts: the chemical enrichment rate at which the gas is polluted by dying stars and the formation rate at which gas is transformed into stars. In reality these two aspects are related, since the more metals are injected into the interstellar medium, the more efficient star formation should be, and also vice versa (e.g. low surface brightness galaxies have low metallicity and low star formation rates). In this paper, we assume that the star formation rate depends solely on the circular velocity of the halo (see Appendix A). We then compute the enrichment of the interstellar medium using accurate nucleosynthesis prescriptions. We refer to Jimenez et al. (1999) for a detailed description of the chemical evolution equations used and the stellar yields.

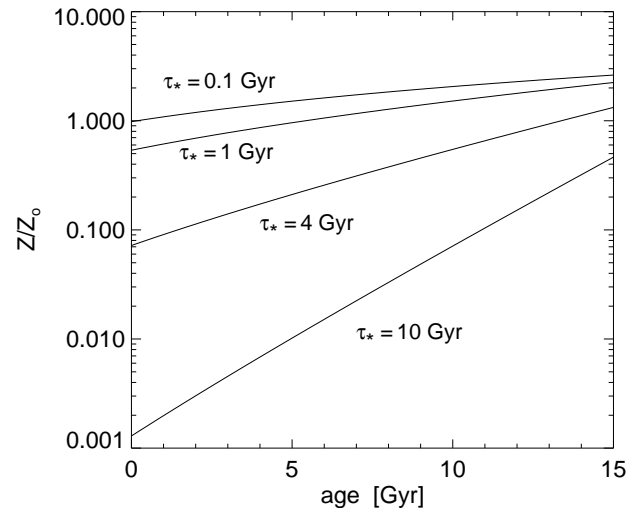


Figure C1. Metallicity evolution for various star formation timescales τ_* .

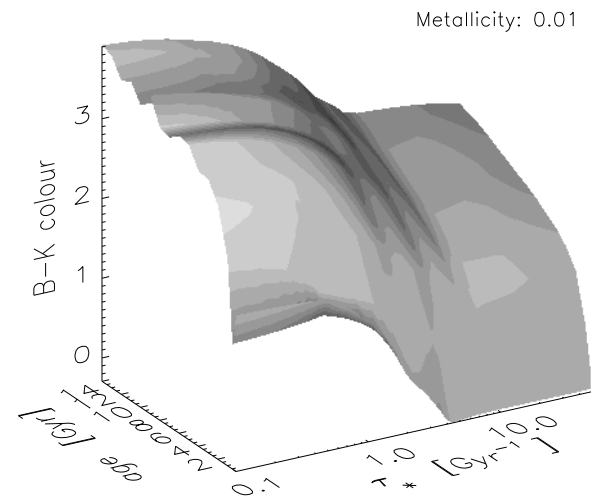


Figure C2. B-K colour for a stellar population with an initial metallicity of 0.01, as a function of age and star formation timescale τ_* .

In principle, one should compute the hydrodynamical evolution of the baryons for each halo and calculate the surface density of the baryonic disc in order to determine the star formation rate as well as the inflow rate and the outflow from supernovae. Since our simulations do not have a hydrodynamical description of the baryonic component, we proceed in a different way. We use the chemical evolution models of Matteucci & Francois (1989), but with a star formation rate given by eq. (A7), thus implicitly assuming a specific disk model. As our star formation rate is similar to that of e.g. Heavens & Jimenez (1999) and Jimenez et al. (1998), this disk model will be close to the disk model of these authors. With this set-up it is possible to obtain a surface that describes τ_* vs. $Z(t)$, where τ_* is given in terms

of V_c by eq. (A8). We show $Z(t)$ for four different values of τ_* in Fig. C1. For a given τ_* and initial Z , a population will evolve with time as described in Appendix A. An example of the B-K colour evolution is shown in Fig. C2.

APPENDIX D: STAR FORMATION BELOW THE N-BODY RESOLUTION LIMIT

The N-body simulation technique has a lower limit on the mass of the haloes identified. In the hierarchical picture these must have formed through merging of haloes with masses below that limit. We thus need to approximate the stellar and gas mass resulting from the evolution along the merger tree below the numerical resolution limit. Both modes of star formation need to be accommodated, with the complication that merging of small-scale structure is relatively frequent at early times. Although both modes will occur intermittently, we approximate the average of all these periodic contributions taken together, by assuming a basic star formation timescale of 0.5 Gyr. We estimate the amount of gas cooled in the sub-tree by considering a single population which has two thirds of the circular velocity of the halo in which the sub-tree terminates, and half its age at the time of formation.

This approximation will be improved upon in future work by linking analytical merger subtrees, obtained using the extended Press-Schechter formalism, to the leaves of the merger tree extracted from the numerical simulation. For the present paper, these subtrees below the N-body resolution limit are not important, as they represent old stellar populations that have faded over many Gyr, and are likely to end up in bulges and centres of elliptical galaxies. They therefore contribute little to the present day luminosities that enter the Tully-Fisher relation and luminosity functions.